



## Enhancing anti-thrombogenicity of biodegradable polyurethanes through drug molecule incorporation

Journal:	<i>Journal of Materials Chemistry B</i>
Manuscript ID	TB-ART-06-2018-001582.R1
Article Type:	Paper
Date Submitted by the Author:	05-Aug-2018
Complete List of Authors:	Xu, Cancan; University of Texas, Bioengineering Kuriakose, Aneetta; University of Texas, Bioengineering Truong, Danh; University of Texas, Bioengineering Punnakitikashem, Primana; University of Texas, Bioengineering Nguyen, Kytai T. ; University of Texas, Bioengineering Hong, Yi; University of Texas, Bioengineering

## Enhancing anti-thrombogenicity of biodegradable polyurethanes through drug molecule incorporation†

Cancan Xu,<sup>a,b</sup> Aneetta E. Kuriakose,<sup>a,b</sup> Danh Truong,<sup>a,b</sup> Primana Punnakitikashem,<sup>a,b</sup> Kytai T. Nguyen,<sup>a,b</sup> and Yi Hong<sup>a,b,\*</sup>

<sup>a</sup> Department of Bioengineering, University of Texas at Arlington, Arlington, TX 76019, USA

<sup>b</sup> Joint Biomedical Engineering Program, University of Texas Southwestern Medical Center, Dallas, TX 75390, USA

† **Electronic supplementary information (ESI) available:** swelling ratio of PU-DPA films in HFIP. See DOI: 10.1039/x0xx00000x

\***Corresponding author:** Yi Hong, [yihong@uta.edu](mailto:yihong@uta.edu), Tel: +1-817-272-0562; Fax: +1-817-272-2251.

## Abstract

Sufficient and sustained anti-thrombogenicity is essential for blood-contacting materials, because blood coagulation and thrombosis caused by platelet adhesion and activation on material surfaces may lead to functional failure and even fatal outcomes. Covalently conjugating anti-thrombogenic moieties into polymer, instead of surface modifying or blending, can maintain the anti-thrombogenicity of polymer at a high level over a time range. In this study, series of randomly crosslinked, elastic, biodegradable polyurethanes (PU-DPA) were synthesized through a one-pot and one-step method from polycaprolactone (PCL) diol, hexamethylene diisocyanate (HDI) and anti-thrombogenic drug, dipyridamole (DPA). The mechanical properties, hydrophilicity, *in vitro* degradation, and anti-thrombogenicity of the resultant PU-DPA polymers can be tuned by altering the incorporated DPA amount. The surface and bulk hydrophilicity of the polyurethanes decreased with increasing hydrophobic DPA amount. All PU-DPA polymers exhibited strong mechanical properties and good elasticity. The degradation rates of the PU-DPAs decreased with increasing DPA content in both PBS and lipase/PBS solutions. Covalently incorporating DPA into the polyurethane significantly reduced the platelet adhesion and activation compared to the polyurethane without DPA, and also can achieve sustained anti-thrombogenicity. The PU-DPA films also supported the growth of human umbilical vein endothelial cells. The attractive mechanical properties, blood compatibility, and cell compatibility of this anti-thrombogenic biodegradable polyurethane indicate that it has a great potential to be utilized for blood-contacting devices, and cardiovascular tissue repair and regeneration.

**Key words:** biodegradable polyurethane, dipyridamole, anti-thrombogenicity, blood-contacting.

## Introduction

Anti-thrombogenicity of biomedical materials remains challenges for blood contacting devices and implants. Platelet adhesion and activation on material surfaces of blood-contacting medical devices and implants, such as stent, vascular graft, artificial organ implants, and hemodialysis equipment, cause thrombotic and thromboembolic complications, which may need further intervention or even cause functional failure or fatal outcomes.<sup>1, 2</sup> For example, large-diameter synthetic vascular grafts (e.g., EXCLUDER<sup>®</sup>, Endurant<sup>®</sup>, and AneuRx<sup>®</sup>) for abdominal aortic aneurysms (AAA) treatment have limb thrombotic occlusion risks up to 7.2%, which appears to be low but usually require further intervention to resolve ischemic symptoms.<sup>3-6</sup> Applications of small-diameter synthetic vascular grafts (inner diameter < 6 mm) have been greatly limited because of their high rates of thrombotic occlusion, which may cause acute failure.<sup>7, 8</sup> Besides, the thrombotic and thromboembolic complications during artificial heart implantation or cardiopulmonary bypass sometimes can be life-threatening.<sup>9, 10</sup> Therefore, it is essential to develop new blood-contacting materials with sufficient and sustained anti-thrombogenicity.

Biodegradable polyurethanes (PUs) have been extensively studied for blood-contacting devices, especially for vascular grafts and stent coatings.<sup>8, 11-13</sup> Surface modifications on biodegradable polyurethanes by anti-thrombogenic moieties (e.g., phosphorylcholine, sulfobetaine, anti-thrombogenic drugs, and heparin) have shown improved anti-thrombogenicity.<sup>11, 14-16</sup> However, such modifications may not have sustained anti-thrombogenicity due to the loss of surface grafted moieties with degradation. These anti-thrombogenic molecules, such as anti-thrombogenic drug, can also be blended with biodegradable PU to achieve anti-thrombogenic PUs. However, the anti-thrombogenicity of the

drug eluting polyurethane scaffold could be gradually weakened and even loss due to the continuous and completed release of anti-thrombogenic drugs from the polyurethane scaffold with time via polymer degradation.<sup>8, 17</sup> To maintain the anti-thrombogenicity of polymer, covalently conjugating the anti-thrombogenic moieties into the polyurethane can achieve an anti-thrombogenic polymer, whose thrombo-resistance can be sustained with degradation. The sulfobetaine was incorporated into the polyurethane backbone and showed markedly reduced thrombogenicity before and after degradation.<sup>17</sup> In our previous study, dipyridamole (DPA), a clinically used anti-thrombogenic drug, was blended with a biodegradable polyurethane and then electrospun into fibrous scaffold, which have shown reduced thrombogenicity.<sup>18</sup> Thus, it is interesting to investigate if covalently incorporating the DPA into the polyurethane can enhance the polymer anti-thrombogenicity without DPA release, and it can provide long-term anti-thrombogenicity..

In this *proof-of-concept* study, biodegradable and elastic polyurethanes with DPA (PU-DPA) were synthesized through a one-pot and one-step method of combining polycaprolactone diol (PCL), hexamethylene diisocyanate (HDI) and DPA with four hydroxyl groups (**Figure 1A**). The obtained polyurethanes have randomly crosslinking structure, and the DPA content can be tuned by varying the molar ratio of DPA to PCL. The chemical structure, mechanical properties and *in vitro* degradation profile of the synthesized PU-DPA polymers were characterized. The blood contact behavior of the PU-DPA films was assessed by hemolysis, and platelet deposition using human whole blood. The *in vitro* cell compatibility of the polyurethane films were investigated by culturing human umbilical vein endothelial cells on PU-DPA films.

## Experimental methods

### Materials

PCL (Mn = 2000, Sigma) was dried overnight to remove residual water in a vacuum oven at 60 °C prior to synthesis. HDI (Sigma) were dehydrated using vacuum distillation before use. Stannous octoate ( $\text{Sn}(\text{Oct})_2$ , Sigma) was dried using 4-Å molecular sieves. Dipyrindamole (DPA, Sigma), dichloromethane (DCM, Sigma), 1,1,1,3,3,3-hexafluoroisopropanol (HFIP, Oakwood Product), ethanol (Decon labs, Inc) hexamethyldisilazane (HMDS, Sigma), Glutaraldehyde (Sigma), osmium tetroxide (Electron Microscopy Science), lipase from *Thermomyces lanuginosus* ( $\geq 100,000$  U/g, Sigma) were used as received.

### Synthesis of polyurethanes incorporating DPA

PU-DPAs were prepared using PCL, HDI and DPA through a one-step/one-pot synthesis method (**Figure 1A**). Briefly, PCL was dissolved in DCM in a 20 ml scintillation vial, followed by addition of DPA with different ratios of DPA to PCL. After vigorous shaking to create a homogenous solution, HDI was added followed by  $\text{Sn}(\text{Oct})_2$  catalyst (2 drops). The mixed solution was poured into a covered Teflon<sup>®</sup> dish, and then placed in an oven at 70 °C for 45 minutes. The dish is then placed in a vacuum oven at 65 °C and allowed to dry overnight. The formed films were removed from the cup, and immersed in 100% ethanol for 24 hours to remove unreacted monomers, such as unreacted free DPA. The films were then placed in the vacuum oven at 65 °C, and dried overnight. The molar ratios of hydroxyl groups in PCL to those in DPA were set as 100:0, 90:10, 80:20 and 70 :30, where were referred to PU-DPA(100:0), PU-DPA(90:10), PU-DPA(80:20) and PU-DPA(70:30), respectively. The theoretical mass fractions

of the DPA in the PU-DPA polymers are 1.4 wt%, 3.1 wt% and 5.2 wt% for PU-DPA(90:10), PU-DPA(80:20), and PU-DPA(70:30), respectively.

### **Polyurethane characterization**

Fourier transform infrared (FT-IR) spectra of the PU-DPA polymers were obtained using a Thermo Nicolet 6700 FT-IR spectrometer (Thermo Fisher Scientific, Waltham, MA). Water contact angle was measured by sessile drop method using a KSV CAM 101 – Optical Contact Angle and Surface Tension Meter (KSV, Helsinki, Finland). Water absorption of PU-DPA polymers (n=3) was measured by immersing a weighed film ( $W_0$ ) in a phosphate buffer solution (PBS, Sigma) at 37 °C for 48 hours and then weighting the wet film ( $W_1$ ) after removing the surface water. The water absorption was calculated as  $(W_1 - W_0)/W_0 \times 100\%$ . To measure the swelling ratio of PU-DPA films in HFIP, the films (n=3) were weighed ( $W_d$ ) and then immersed in HFIP at room temperature for 24 and 48 hours. At each predetermined time point, the films were weighted as  $W_s$ . The swelling ratio in HFIP was calculated as  $(W_s - W_d)/W_d \times 100\%$ .

Mechanical tensile testing was carried on the polymer films by using 2 x 20 mm strips cut from the films. All testing (n=6) was done using MTS Insight mechanical tester (MTS System, Minneapolis, MN) fitted with a 500 N load cell (Model 56932701, MTS System, Minneapolis, MN). Testing was done at room temperature with a crosshead speed of 10 mm/min. Cyclic stretching was conducted by stretching the PU-DPA films (2 x 20 mm, n=3) to maximum strain of 30% and releasing back to the initial length for 10 cycles at a constant rate of 10 mm/min.<sup>19</sup>

### ***In vitro* hydrolytic and enzymatic degradation**

Polymer degradation was evaluated by weight loss of the films under hydrolytic and enzymatic conditions. Polymer films were cut to approximately 30 mg pieces and weighed for each piece ( $W_0$ ). For hydrolytic conditions, weighed polymer films were immersed in 10 ml of phosphate buffer solution (PBS) at 37 °C. At the prescribed time points, samples are removed and rinsed 3x with deionized water and dried in vacuum oven at 65 °C for three days followed by weighing ( $W_1$ ). For enzymatic conditions, the weighed polymer films are immersed in 2 ml 100 U lipase/PBS solution in a 20 ml glass vial. The glass vials are placed in 37 °C, and fresh lipase/PBS are replaced every two days. At each time points, samples were removed, rinsed 3x with deionized water, and dried in vacuum oven at 65°C for three days followed by weighing ( $W_1$ ). The mass remaining for calculated by  $W_1/W_0 \times 100\%$ . Three samples were used for each polymer at each time point.

### **Hemolysis and platelet deposition of PU-DPA films**

The hemolysis assay on PU-DPA materials was processed as previously described.<sup>20</sup> Human blood was collected from healthy individuals into acid citrate dextrose (ACD) anticoagulant tubes using venipuncture and was handled following methods approved by the Institutional Review Board at the University of Texas at Arlington. Following which, the blood was diluted to 2% (v/v) using saline solution (0.9% NaCl (w/v)), and 200 $\mu$ L of it was transferred on to 6mm diameter polymeric disks and incubated for 2 hours at 37°C. The samples were then centrifuged at 1000 g for 10 minutes, and supernatant was collected to measure the absorbance at 545nm on a UV/vis spectrophotometer (Infinite M200 plate reader, Tecan, Durham, NC). The



blood diluted using deionized (DI) water and saline served as positive and negative controls, respectively. The percentage of hemolysis was calculated using the equation below:

$$\% \text{ Hemolysis} = \frac{\text{Sample OD} - \text{Negative control OD}}{\text{Positive control OD} - \text{Negative control OD}} \times 100\%$$

Anti-thrombogenicity of PU-DPA films was evaluated by platelet deposition. Briefly, the human whole blood was centrifuged at 120 g for 12 minutes to obtain platelet-rich plasma (PRP), which was incubated with PU-DPA samples before and after 14 days of enzymatic degradation and glass (6mm in diameter) for 1 hour at 37°C. The samples were then rinsed 3 times with PBS, and deposited platelets were then lysed with 1% Triton X-100 for 30 minutes at 37°C. The amount of lactate dehydrogenase (LDH) released by the deposited platelets were quantified using LDH assays following manufacturer's instructions (Clonetech, Mountain View, CA). In another parallel study, to observe the platelet deposition and aggregation, the PRP treated samples were fixed in 2% glutaraldehyde solution for overnight, stained with 1% osmium tetroxide for 2 hours, and dehydrated a series of ethanol solution with concentrations 50%, 70%, 95% and 100% (v/v) for 10 minutes each step. The samples were further dried using series of ethanol-HMDS solutions of ratios 2:1, 1:1 and 1:2 for 15 minutes each step, then sputter-coated with silver and imaged on a SEM (Hitachi S-3000N).

### ***In vitro* endothelial cell culture**

Human umbilical vein endothelial cells (HUVECs, ATCC, Manassas, VA) were seeded at a density of 10,000 cells/cm<sup>2</sup> onto the surface of polymer disks (6mm in diameter) and cultured for predetermined time points using Vasculife basal medium supplemented with growth factors (Vasculife VEGF lifefactors kit, Lifeline Cell Technologies, Frederick, MD). The cell

culture medium was fully refreshed alternate days. The tissue-cultured polystyrene (TCPS) served as a control. At each time point, the cellular viabilities ( $n = 4$ ) were measured using MTS assays (Promega, WI) following manufacturer's instructions, and the cellular viability was expressed as a percentage relative to the control TCPS at day 1. The absorbance for the cells cultured on the control TCPS at day 1 was set as 100%. In addition, the morphology of HUVECs on the polymer film surface was also observed under SEM after the fixation and dehydration as described above.

### **Statistical analysis**

Unless specified, all results were expressed as mean  $\pm$  standard deviation. To determine the blood contact evaluation of PU-DPA films, we performed a statistical analysis using one-way ANOVA followed by post-hoc Tukey testing. Two-way ANOVA was utilized followed by post-hoc Sidak testing to observe difference in cellular growth after 1 and 3 days of culture. All these data analysis was conducted in GraphPad Prism (GraphPad Software Inc, CA) and a statistically significant difference was considered when  $p < 0.05$ .

## **Results and discussion**

### **Characterization of PU-DPA films**

The synthesized polyurethane with DPA incorporation looks yellow and transparent due to the intrinsic yellow color of DPA, while the PU without DPA is colorless and transparent (**Figure 1B**). The chemical structures of PU-DPA polymers were verified by FTIR spectra (**Figure 2**). The characteristic peaks of the polyurethanes were located at  $3350\text{ cm}^{-1}$  (N-H stretching of urethane groups),  $2930\text{ cm}^{-1}$  and  $2870\text{ cm}^{-1}$  (symmetric and asymmetric C-H

stretching), and  $1730\text{ cm}^{-1}$  (C=O stretching of urethane groups).<sup>21</sup> The specific peak for DPA was located at  $1530\text{ cm}^{-1}$  corresponding to the aromatic C-C symmetric stretching,<sup>22</sup> whose intensity increased with increasing DPA amount in the polymer.

The surface and bulk hydrophilicities of the PU-DPA films were characterized by water contact angle and water absorption, respectively (**Table 1**). The water contact angle increased with increasing DPA content. The PU-DPA (100:0) without DPA had the smallest contact angle at  $89\pm 3^\circ$ , while the PU-DPA(70:30) with the highest DPA amount had the largest contact angle at  $99\pm 4^\circ$  ( $p < 0.05$ ). The addition of DPA into the polyurethane can also reduce polymer water absorption. The PU-DPA (100:0) had the highest water absorption at  $9\pm 1\%$ , while the PU-DPA(70:30) had the lowest water absorption at  $3\pm 1\%$  ( $p < 0.05$ ). The increasing water contact angle and decreasing water absorption with increased DPA amount in the polyurethane indicated the increased surface and bulk hydrophobicity of the PU-DPA films, which were both attributed to the hydrophobic nature of the DPA.<sup>23</sup> The swelling ratio of PU-DPA films in HFIP (**Figure S1 in the ESI†**) decreased significantly with increased DPA amounts, showing the increased crosslinking degree of the PU-DPA polymer network, which is relevant to the polymer mechanical properties.

### **Mechanical properties of PU-DPA films**

The typical stress-strain curves of PU-DPA films were shown in **Figure 3A**. In **Table 1**, the PU-DPA(80:20) had the highest tensile strength ( $25.4\pm 1.2\text{ MPa}$ ) compared to the PU-DPA(100:0) ( $15.3\pm 0.3\text{ MPa}$ ), PU-DPA(90:10) ( $15.0\pm 2.6\text{ MPa}$ ) and PU-DPA(70:30) ( $20.3\pm 1.5\text{ MPa}$ ). The initial moduli of the PU-DPA films increased with rising DPA contents, ranging from  $3.1\pm 0.7\text{ MPa}$  [PU-DPA(100:0)] to  $4.4\pm 0.1\text{ MPa}$  [PU-DPA(70:30)]. The higher DPA content may

lead to higher crosslinking degree, which was associated with stronger and stiffer materials.<sup>24</sup> The other reason was that the increasing DPA/PCL ratio would result in the increase of the hard segment in the crosslinked PU, which also could induce the initial modulus increase. No significant difference on the breaking strain was observed between the PU-DPA(100:0) (1157±109%), PU-DPA(90:10) (1009±64%), and PU-DPA(70:30) (1107±47%) ( $p > 0.05$ ). However, the PU-DPA(70:30) film had the lowest strain at 829±55% ( $p < 0.05$ ) because of its highest crosslink degree. It is notable that the tensile strength of PU-DPA(70:30) (20.3±1.5 MPa) was lower than that of PU-DPA(80:20) (25.4±1.2 MPa). The polymer mechanical strength is relevant to various factors, such as microphase separation and crystallization, which may be interfered by DPA content. On the other hand, the shorter reaction time (45 min) and lower reaction temperature (70 °C) for PU-DPA synthesis may result in relatively lower crosslinking degree, which led to relatively lower polymer initial modulus (< 5 MPa) compared to previously reported crosslinked PCL based polyurethanes [(7.2-33.8 MPa, reaction taken place at 90 °C for 6 h)<sup>25</sup> and (40.92 MPa, reaction taken place at 85 °C for 21 h)]<sup>26</sup>.

The high elasticity of the PU-DPA polymers was verified by the cyclic stretching of PU-DPA films at a maximum strain of 30% (**Figure 3B**). All groups had a large hysteresis loop in the first cycle, followed by much smaller hysteresis loops in the next nine cycles. All groups showed small irreversible deformations (<5%) at 30% strain, indicating the good elasticity of the PU-DPA films. It may be attributed to the microphase separation of polyurethane nature and the crosslinking network structure.

### ***In vitro* degradation of PU-DPA polymers**

The PU-DPA hydrolytic and enzymatic degradation kinetics in PBS and lipase/PBS solution were shown in **Figure 4A and 4B**, respectively. For hydrolytic degradation (**Figure 4A**), all the polymers demonstrated slow degradation rates within 8 weeks. The PU-DPA(100:0) had a significantly higher mass loss ( $2.8 \pm 1.8\%$ ) compared to PU-DPA(90:10) ( $1.5 \pm 0.5\%$ ), PU-DPA(80:20) ( $1.4 \pm 1.0\%$ ), and PU-DPA(70:30) ( $1.4 \pm 0.3\%$ ) ( $p < 0.05$ ) after 8 weeks of hydrolysis. The hydrolytic degradation of all PU-DPA polymers were slow because PCL is a slowly degrading polymer,<sup>27</sup> and our result was consistent with previous studies.<sup>28-31</sup> The addition of DPA into the polyurethane would further reduce its hydrolysis rate because the hydrophobic characteristics of DPA and the formed crosslinking network could enhance the polymer structure stability and make polymer resistant to both hydrolytic and enzymatic degradation.<sup>32</sup> The enzymes existing in body and the host response (e.g., macrophage accumulation) could accelerate the polymer degradation.<sup>33</sup> The polymer enzymatic degradation in lipase/PBS solution presented similar trends as that in PBS, however, their enzymatic degradation rates were correspondingly higher than those in PBS (**Figure 4B**). In the lipase/PBS solution, the PU-DPA(100:0) had the highest degradation rate (21.8 $\pm$ 10.4% mass remaining at day 14), while the PU-DPA(70:30) had the lowest degradation rate (98.6 $\pm$ 0.7% mass remaining at day 14). SEM images further confirmed that the PU-DPA films were enzymatically degraded by observing their surface morphology changes (**Figure 4C**). The surfaces of all solid polymer films were smooth and homogeneous prior to degradation. After 14 days of enzymatic degradation, the film surfaces showed roughness and even cracks. Hydrolase lipase is primarily used to catalyze the ester bond break-down with hydrolysis.<sup>34</sup> The higher DPA content was associated with lower PCL content, indicating less ester bonds existed. In addition, the crosslinking network can resist

the water penetration into the polymer, which could further inversely affect its enzymatic degradation.<sup>32</sup>

### **Hemolysis and platelet deposition of PU-DPA films**

The blood contact behaviors of the PU-DPA materials were assessed through hemolysis, platelet adhesion, and platelet aggregation. Hemolysis assay is one of indispensable initial tests to determine the adverse effects of polymeric biomaterials on red blood cells (RBCs) *in vivo*. If the material is hemo-incompatible, it disrupts RBCs, leading to the release of its intercellular contents including hemoglobin in to plasma that could eventually result in critical consequences like anemia, jaundice, acute renal failure, and death.<sup>35, 36</sup> Based on ISO standard practice for assessment of hemolytic properties of materials,<sup>37</sup> a biomaterial is classified as nonhemolytic, slightly hemolytic, or hemolytic when the percentage of hemoglobin released after incubating the whole blood with biomaterial was 0%-2%, 2%-5, or >5%, respectively. The results obtained for hemolysis of ACD blood with PU-DPA materials were shown in **Figure 5A**. All of the polymers observed to cause less than 2% of hemolysis with statistical difference ( $p>0.05$ ), although there existed a trend of hemolysis reduction with the increase of the DPA amount in the polyurethane. This indicated that PU-DPA materials are non-hemolytic, and hence it may be suitable for the desired vascular applications.

The platelet adhesion and aggregation on to biomaterial implant determines its anti-thrombogenic potential. In response to the proteins adsorbed on to foreign surface, the platelets interact with them via its integrin receptors and turn activated. These activated platelets can further activate many kinds of coagulation factors, promoting the formation of thrombosis and aggregation. Therefore, the prevention of platelet adhesion to the biomaterial surface is crucial to

improve its blood compatibility. As shown in **Figure 5B**, with increasing amounts of DPA incorporated into the polyurethanes resulted in lower amounts of platelet deposition. However, the substantially reduced amount of platelet deposition on the material surface was observed only for PU-DPA(70:30) compared to PU film without DPA. Furthermore, in agreement to LDH assays that quantified the platelet adhesion, SEM images showed similar trend in platelet deposition on the PU films. These images in **Figure 5C** revealed that the platelets deposited on to PU films with DPA have round morphology indicative for inactivated platelets, whereas those on PU-DPA(100:0) mostly appeared irregular with fully spread pseudopodia that represented the activated state of platelets.<sup>38</sup> To investigate the retention of the anti-thrombogenicity for the enzyme-degraded PU-DPA films, human platelet-rich plasma was contacted with PU-DPA films after 14 days of enzymatic degradation (**Figure 6**). Significantly reduced platelet deposition was found on the enzyme-degraded PU-DPA(70:30) film compared with the degraded PU-DPA (100:0) and glass (**Figure 6A**). SEM images quantitatively confirmed the LDH results (**Figure 6B**), in which less platelet deposition was found on the enzyme-degraded PU-DPA(70:30) films than those on degraded PU-DPA(100:0) and glass. These results showed that covalent incorporation of DPA into the polyurethane can reduce the platelet deposition, decreased the propensity of polymeric surface to activate adherent platelets and maintained the anti-thrombogenicity over a long term with degradation, thereby improving their anti-thrombogenicity with endurance.

The mechanism of action of conjugated DPA on the anti-platelet activity is still not clear. We envisage that DPA molecules incorporated into polymeric films might be recognized by the anchoring molecules on the platelet's surface, leading to increase in intracellular levels of cyclic adenosine monophosphate (cAMP) and cyclic guanine monophosphate (cGMP) within platelets

<sup>39, 40</sup>. It is also plausible that DPA grafting changes the physical properties of polymeric surface, which in turn affects the interaction of plasma proteins with the material and subsequent platelet responses. For instance, Wu et al.<sup>41</sup> analyzed the effects of surface properties of various types of PUs, and observed lower platelet adhesion on hydrophilic PU than its hydrophobic counterparts due to ultralow adsorption of fibrinogen from plasma to the material surface. Interestingly, the hydrophobic PUs with relatively high fibrinogen adsorption also exhibited lower platelet adhesion. The studies concluded that the surface chemistry dictates the fibrinogen conformation adsorbed on to material, and thereby exposing the platelet binding domains affecting their adhesion and activation.<sup>41, 42</sup> As previously noted, the PU-DPA exhibited increasing hydrophobicity with increasing contents of DPA, with PU-DPA (70:30) having the highest contact angle of  $99\pm 4^\circ$  compared to PU-DPA (100:0) with  $89\pm 3^\circ$ . Therefore, the role of surface characteristics of the PU-DPA samples on the observed platelet response cannot be eliminated. Hence, further studies will be required to investigate the mechanism how PU-DPA materials enhanced its anti-thrombogenic characteristics.

### ***In vitro* HUVEC viability on PU-DPA polymers**

Endothelial cell layer formation on materials is a gold standard to offer a long-term anti-thrombosis for implanted blood-contacting medical devices. The ability of PU-DPA films to support endothelial cell growth was exhibited in **Figure 7**. Cellular viability was determined using MTS assays after 1 and 3 days of culture on PU-DPA films (**Figure 7A**). Cells grown on TCPS served as the control. Significantly lower percentage of endothelial cells adhered and proliferated on the polymeric films compared to TCPS for both the time points ( $p < 0.0001$ ). This reduction in cell performance on the PU-DPA samples is due to its hydrophobic nature,



which can be improved by numerous surface modification strategies including physical modification by plasma treatment, etching, gamma irradiation, X-ray treatment;<sup>43-45</sup> chemical modification by grafting hydrophilic materials;<sup>46-49</sup> and bioactive modification by immobilization of endothelial cell adhesive peptides on to polymeric surface.<sup>50-52</sup> However, cellular viabilities on PU-DPA (80:20) and PU-DPA (70:30) were significantly higher than that for PU-DPA (90:10) and PU-DPA (100:0) at day 3 ( $p < 0.05$ ), which was also qualitatively verified by the electron micrographs of spread HUVECs seeded on PU-DPA films (**Figure 7B**). In addition, HUVECs proliferation was observed for both PU-DPA (80:20) and PU-DPA (70:30) as their cell viabilities at day 3 were significantly higher than at day 1 ( $p < 0.05$ ). In our previous work, it was observed that DPA releasing biodegradable elastic PU (BPU) scaffolds improved human aortic endothelial cell growth over 7 days of culture compared to BPU scaffolds alone.<sup>20</sup> Aldenhoff et al.<sup>53</sup> observed the DPA immobilized PU based vascular graft supported the formation of endothelial-like cell lining in a sheep carotid artery model. In terms of these reports and our results implies that DPA involvement may support the endothelial cell growth. It would make the PU-DPA polymer attractive as a good blood-contacting material candidate because it has good anti-thrombogenicity without adverse effect on endothelialization.

There are some limitations existing in this study. First, the polymer mechanical properties can not only be tuned by altering the feeding ratio of DPA to PCL, but also by altering the reaction time and temperature during the PU-DPA synthesis. In this study, the 45 min of reaction time at 70°C might be short as discussed above. However, low-initial modulus polymers are also important for biomedical engineering applications. It may be able to utilized as porous scaffolds to repair soft and elastic human tissues with low initial moduli.<sup>54, 55</sup> Secondly, the introduction of DPA significantly reduced the biodegradation rate of the polyurethane due to the increased

hydrophobicity and network structure. To accelerate the biodegradability of PU-DPA, polyester diols with higher molecular weights which contain more lipase-susceptible ester bonds can be used as the soft segment in the polyurethane structure,<sup>54</sup> instead of the PCL (Mn=2000) diol. Additionally, after processing the PU-DPA polymer into 3D porous scaffold, its biodegradability may be enhanced because of the porous structure and greatly increased surface area which can allow higher water penetration into the polymer network and more interaction between water and polymer chains.<sup>56, 57</sup> Thirdly, the material characterizations focused on 2D films, which may provide solid evidence for anti-thrombogenic coating applications. However, it is not sufficient for 3D porous scaffold use. In the future, we will further evaluate in detail about the mechanical properties and biological functions of the PU-DPA based 3D materials *in vitro* and *in vivo*.

## Conclusions

A family of biodegradable, elastic and crosslinked polyurethanes with anti-thrombogenic drug was synthesized using a simple one step/one pot method. The crosslinked polyurethanes had good elasticity, and their mechanical and degradation properties can be tuned by altering the feeding ratio of DPA to PCL segments. The resultant anti-thrombogenic polyurethanes significantly reduced the platelet deposition on polymer surfaces before and after enzymatic degradation, and also supported the growth of HUVECs. These promising characters of the anti-thrombogenic and biodegradable elastomer show its great potential to be used as a blood-contacting biomaterial.

## Conflicts of interest

There are no conflicts to declare.

## **Acknowledgements**

We greatly appreciate the partial financial support from CAREER award 1554835 (YH) from the National Science Foundation, and R21HD090680 (YH), R01 HL118498 (KTN), T32 HL134613 (KTN, and AEK is a fellow of NIH T32) from the National Institutes of Health.

## References

- 1 O. A. Hamad, J. Bäck, P. H. Nilsson, B. Nilsson and K. N. Ekdahl, *Adv Exp Med Biol.*, 2012, **946**, 185.
- 2 M. B. Gorbet and M. V. Sefton, *Biomaterials*, 2004, **25**, 5681.
- 3 E. M. Faure, J. P. Becquemin, F. Cochenec, R. G. Monaco, M. Ferreira, R. Fitridge, N. Boyne, S. Dubenec, M. Grigg and P. Mwapatayi, *J Vasc Surg.*, 2015, **61**, 1138 e2.
- 4 A. Carroccio, P. L. Faries, N. J. Morrissey, V. Teodorescu, J. A. Burks, E. C. Gravereaux, L. H. Hollier and M. L. Marin, Predicting iliac limb occlusions after bifurcated aortic stent grafting: anatomic and device-related causes. *J Vasc Surg.*, 2002, **36**, 679.
- 5 R. A. Stokmans, J. A. Teijink, T. L. Forbes, D. Böckler, P. J. Peeters, V. Riambau, P. D. Hayes and M. R. van Sambeek, *Eur J Vasc Endovasc Surg.*, 2012, **44**, 369.
- 6 M. Kim, M. G. Kim, W. C. Kang, P. C. Oh, J. Y. Lee, J. M. Kang, W. J. Chung and E. K. Shin, *Korean Circ J.*, 2016, **46**, 727.
- 7 H. Kurobe, M. W. Maxfield, S. Tara, K. A. Rocco, P. S. Bagi, T. Yi, B. Udelsman, Z. W. Zhuang, M. Cleary, Y. Iwakiri, C. K. Breuer and T. Shinoka, *PLoS One.*, 2015, **10**, e0120328.
- 8 Y. Hong, S. H. Ye, A. Nieponice, L. Soletti, D. A. Vorp and W. R. Wagner, *Biomaterials*, 2009, **30**, 2457.
- 9 R. L. Bick, *Pathology.*, 2003, **35**, 458.
- 10 D. K. Tempe, P. Lalwani, K. Chaudhary, H. S. Minas and A. S. Tomar, *J Anaesthesiol Clin Pharmacol.*, 2017, **33**, 117.

- 11 L. Soletti, A. Nieponice, Y. Hong, S. H. Ye, J. J. Stankus, W. R. Wagner and D. A Vorp, *J Biomed Mater Res A.*, 2011, **96**, 436.
- 12 W. Chen, C. di Carlo, D. Devery, D. J. McGrath, P. E. McHugh, K. Kleinsteinberg, S. Jockenhoevel, W. E. Hennink and R. J. Kok, *Int J Pharm.*, 2017, pii: S0378-5173(17)30996.
- 13 Q. Guo, P. T. Knight and P. T. Mather, *J Control Release.*, 2009, **137**, 224.
- 14 Y. Jiang, H. Qingfeng, L. Baolei, S. Jian and L. Sicong, *Colloids Surf B Biointerfaces.*, 2004, **36**, 19.
- 15 G. A. Abraham, A. A. de Queiroz and J. San Román, *J, Biomaterials*, 2002, **23**, 1625.
- 16 Z. Zhou and M. E. Meyerhoff, *Biomaterials*, 2005, **26**, 6506.
- 17 S. H. Ye, Y. Hong, H. Sakaguchi, V. Shankarraman, S. K. Luketich, A. D'Amore and W. R. Wagner, *ACS Appl Mater Interfaces.*, 2014, **6**, 22796.
- 18 P. Punnakitikashem, D. Truong, J. U. Menon, K. T. Nguyen and Y. Hong, *Acta Biomater.*, 2014, **10**, 4618.
- 19 X. J. Loh, K. K. Tan, X. Li and J. Li, *Biomaterials*, 2006, **27**, 1841.
- 20 P. Punnakitikashem, D. Truong, J. U. Menon, K. T. Nguyen and Y. Hong, *Acta Biomater.*, 2014, **10**, 4618.
- 21 M. C. Delpech and G. S. Miranda, *Cent Eur J Eng.*, 2012, **2**, 231.
- 22 S. B. Vepuri, H. Devarajegowda and M. E. Soliman, *J. Mol. Struct.*, 2016, **1105**, 194.
- 23 Y. Tang, S. Y. Liu, S. P. Armes and N. C. Billingham, *Biomacromolecules*, 2003, **4**, 1636.
- 24 Q. Fan and C. Xiao, *Polym Compos.*, 2008, **29**, 758.
- 25 A. Güney and N. Hasirci, *J. Appl. Polym. Sci.*, 2014, **131**, 39758.

- 26 S. Y. Lee, S. C. Wu, H. Chen, L. L. Tsai, J. J. Tzeng, C. H. Lin and Y. M. Lin, *Biomed Res Int.*, 2018, **2018**, 3240571.
- 27 M. Vert, *J Mater Sci Mater Med.*, 2009, **20**, 437.
- 28 C. Xu, Y. Huang, J. Wu, L. Tang and Y. Hong, *ACS Appl Mater Interfaces.*, 2015, **7**, 20377.
- 29 C. Xu, G. Yopez, Z. Wei, F. Liu, A. Bugarin and Y. Hong, *J Biomed Mater Res A.*, 2016, **104**, 2305.
- 30 C. Xu, Y. Huang, G. Yopez, Z. Wei, F. Liu, A. Bugarin, L. Tang and Y. Hong, *Sci Rep.*, 2016, **6**, 34451.
- 31 Y. Hong, S. H., Ye, A. L. Pelinescu and W. R. Wagner, Synthesis, characterization, and paclitaxel release from a biodegradable, elastomeric, poly (ester urethane) urea bearing phosphorylcholine groups for reduced thrombogenicity. *Biomacromolecules*, 2012, **13**, 3686.
- 32 L. Yang, J. Li, M. Li and Z. Gu, The in vitro and in vivo degradation of cross-linked poly (trimethylene carbonate)-based networks. *Polymers*, 2016, **8**, 151.
- 33 M. Tracy, K. Ward, L. Firouzabadian, Y. Wang, N. Dong, R. Qian and Y. Zhang, *Biomaterials*, 1999, **20**, 1057.
- 34 Y. Tokiwa and T. Suzuki, *Nature*, 1977, **270**, 76.
- 35 J. U. Menon, A. Kuriakose, R. Iyer, E. Hernandez, L. Gandee, S. Zhang, M. Takahashi, Z. Zhang, D. Saha and K. T. Nguyen, *Sci Rep.*, 2017, **7**, 13249.
- 36 H. Jeong, J. Hwang, H. Lee, P. T. Hammond, J. Choi and J. Hong, *Sci Rep.*, 2017, **7**, 9481.

- 37 B. I. Cerda-Cristerna, H. Flores, A. Pozos-Guillén, E. Pérez, C. Sevrin and C. Grandfils, *J Control Release.*, 2011, **153**, 269.
- 38 W. Okrój, M. Walkowiak-Przybyło, K. Rośniak-Bak, L. Klimek and B. Walkowiak, *Acta Bioeng Biomech.*, 2009, **11**, 45.
- 39 Y. Aldenhoff and L. H. Koole, *Eur Cell Mater.*, 2003, **5**, 61; discussion 67.
- 40 H. H. Kim and J. K. Liao, *Arterioscler Thromb Vasc Biol.*, 2008, **28**, s39.
- 41 Y. Wu, F. I. Simonovsky, B. D. Ratner and T. A. Horbett, *J Biomed Mater Res A.*, 2005, **74**, 722.
- 42 L. Zhang, B. Casey, D. K. Galanakis, C. Marmorat, S. Skoog, K. Vorvolakos, M. Simon and M. H. Rafailovich, *Acta Biomater.*, 2017, **54**, 164.
- 43 S. De, R. Sharma, S. Trigwell, B. Laska, N. Ali, M. K. Mazumder and J. Mehta, *J Biomater Sci Polym Ed.*, 2005, **16**, 973.
- 44 A. J. Melchiorri, N. Hibino and J. P. Fisher, *Tissue Eng Part B Rev.*, 2013, **19**, 292.
- 45 I. Adipurnama, M. C. Yang, T. Ciach and B. Butruk-Raszeja, *Biomater Sci.* 2016, **5**, 22.
- 46 F. Noorisafa, A. Razmjou, N. Emami, Z. X. Low, A. H. Korayem and A. A. Kajani, *J Exp. Nnanosci.*, 2016, **11**, 1087.
- 47 S. H. Hsu and W. C. Chen, *Biomaterials*, 2000, **21**, 359.
- 48 C. He, M. Wang, X. Cai, X. Huang, L. Li, H. Zhu, J. Shen and J. Yuan, *Appl. Surf. Sci.*, 2011, **258**, 755.
- 49 J. Fang, J. Zhang, J. Du, Y. Pan, J. Shi, Y. Peng, W. Chen, L. Yuan, S. H. Ye, W. R. Wagner, M. Yin and X. Mo, *ACS Appl Mater Interfaces.*, 2016, **8**, 14442.
- 50 L. J. Taite, P. Yang, H. W. Jun and J. L. West, *J Biomed Mater Res B Appl Biomater.*, 2008, **84**, 108.

- 51 W. S. Choi, J. W. Bae, Y. K. Joung, K. D. Park, M. H. Lee, J. C. Park and I. K. Kwon, *Macromol. Res.*, 2009, **17**, 458.
- 52 X. Ding, W. Chin, C. N. Lee, Neng, J. L. Hedrick and Y. Y. Yan, *Adv Healthc Mater.* 2018, **7**, 1700944.
- 53 Y. B. Aldenhoff, F. H. van Der Veen, J. ter Woorst, J. Habets, L. A. Poole-Warren and L. H. Koole, *J Biomed Mater Res.*, 2001, **54**, 224.
- 54 C. Xu, Y. Huang, L. Tang and Y. Hong, *ACS Appl Mater Interfaces.*, 2017, **9**, 2169.
- 55 Z. Ma, Y. Hong, D. M. Nelson, J. E. Pichamuthu, C. E. Leeson and W. R. Wagner, *Biomacromolecules*, 2011, **12**, 3265.
56. P. Musto, G. Ragosta, G. Scarinzi, and L. Mascia, *J. Polym. Sci., Part B: Polym. Phys.* 2002, **40**, 922.
57. M. Spagnuolo and L. Liu, *ISRN Nanotechnol.*, 2012, **2012**, 627420.



## Captions

**Table 1.** Polymer film characterization.

**Figure 1.** PU-DPA synthesis. (A) Synthesis scheme of PU-DPA from polycaprolactone (PCL) diol, hexamethylene diisocyanate (HDI) and anti-thrombogenic drug, dipyridamole (DPA). (B) Digital images to show the color change with PU-DPA films after DPA incorporation.

**Figure 2.** FT-IR spectra of PU-DPA polymers to verify their chemical structures.

**Figure 3.** Mechanical properties of PU-DPA. (A) Typical stress-strain curves of PU-DPA films. (B) Images to show the PU-DPA(70:30) film is highly stretchable. (C) Cyclic stretching curves of PU-DPA polymers (n=3) at 30% strain to exhibit their high elasticity.

**Figure 4.** Mass remaining for PU-DPA films (n=3) in (A) PBS up to 8 weeks and (B) 100 U/mL lipase/PBS up to 14 days at 37 °C. \* represents significantly different groups ( $p < 0.05$ ). (C) Scanning electron micrographs of the surface morphologies of PU-DPA films before and after enzymatic degradation for 14 days.

**Figure 5.** Hemocompatibility assessment of PU-DPA films. (A) Percentage of red blood cells lysis after 2-hour exposure of whole blood with PU-DPA films (n = 4). DI water and saline diluted blood served as positive and negative control respectively. Glass is used for a comparison for blood testing studies. (\* denotes  $p < 0.05$  for significant difference with respect to glass, PU-DPA(100:0), PU-DPA(90:10), PU-DPA(80:20) and PU-DPA(70:30)), (B) Amount of LDH released by triton treated platelets after adhering on to PU-DPA films in 1-hour incubation at 37°C (n=5, \$ and # denote  $p < 0.05$  for

significant difference with respect to PU-DPA (100:0) and glass, respectively); and (C) SEM images to show platelet deposition and morphology on PU-DPA films.

**Figure 6.** Blood platelets deposition on enzymatically degraded PU-DPA films. (A) Amount of LDH released by triton treated platelets deposited on PU-DPA films after 1-hour incubation at 37°C (n=5, \$ and # denote  $p < 0.05$  for significant difference with respect to PU-DPA (100:0) and glass, respectively); and (B) SEM images to show platelet deposition and morphology on enzymatically degraded PU-DPA films (14 days).

**Figure 7.** *In vitro* HUVEC growth on PU-DPA films. (A) Cell viability measured by MTS assay to show HUVECs growth on the surfaces of PU-DPA films up to 3 days (n = 4). TCPS surface served as the control. (B) SEM images showed HUVECs morphology on surfaces of PU-DPA films at day 3. (\* denotes  $p < 0.05$  for significant difference within the groups after 1 and 3 days of culture).

**Table 1.** Polymer film characterization\*

Samples	Contact angle (deg)	Water absorption (%)	Tensile strength (MPa)	Initial modulus (MPa)	Breaking strain (%)
PU-DPA(100:0)	89±3 <sup>a</sup>	9±1 <sup>a</sup>	15.3±0.3 <sup>a</sup>	3.1±0.7 <sup>a</sup>	1157±109 <sup>a</sup>
PU-DPA(90:10)	95±4 <sup>a,b</sup>	7±1 <sup>b</sup>	15.0±2.6 <sup>a</sup>	3.6±0.4 <sup>a,b</sup>	1009±64 <sup>a</sup>
PU-DPA(80:20)	97±5 <sup>b</sup>	5±1 <sup>c</sup>	25.4±1.2 <sup>b</sup>	3.6±0.1 <sup>b</sup>	1107±47 <sup>a</sup>
PU-DPA(70:30)	99±4 <sup>b</sup>	3±1 <sup>d</sup>	20.3±1.5 <sup>c</sup>	4.4±0.1 <sup>c</sup>	829±55 <sup>b</sup>

\*a, b, c and d denote statistical differences between groups for each characterization.

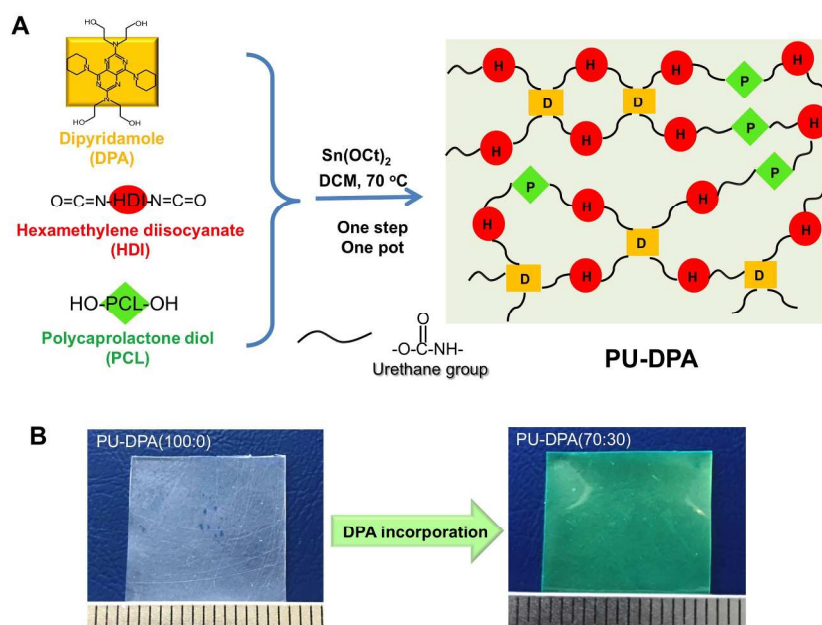


**Figure 1**

Figure 1. PU-DPA synthesis. (A) Synthesis scheme of PU-DPA from polycaprolactone (PCL) diol, hexamethylene diisocyanate (HDI) and anti-thrombogenic drug, dipyridamole (DPA). (B) Digital images to show the color change with PU-DPA films after DPA incorporation.

874x656mm (72 x 72 DPI)

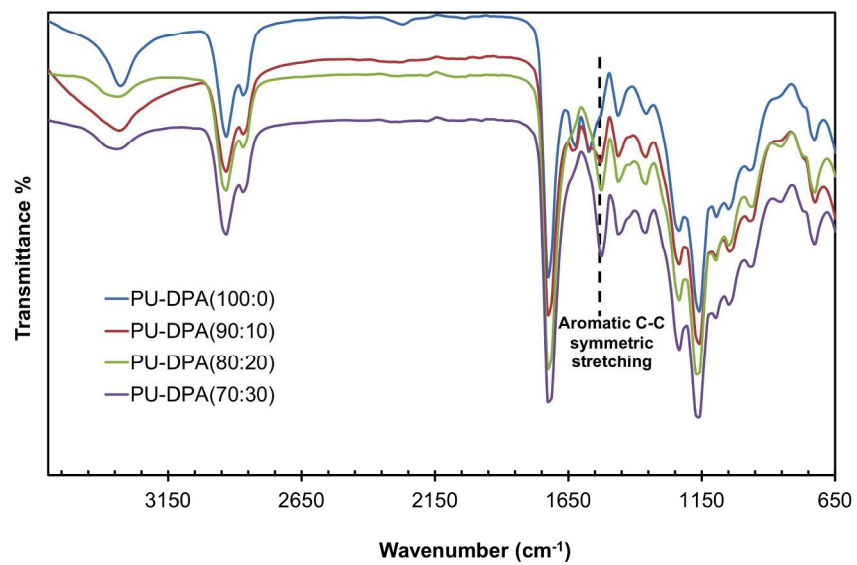


**Figure 2**

Figure 2. FT-IR spectra of PU-DPA polymers to verify their chemical structures.

874x656mm (72 x 72 DPI)

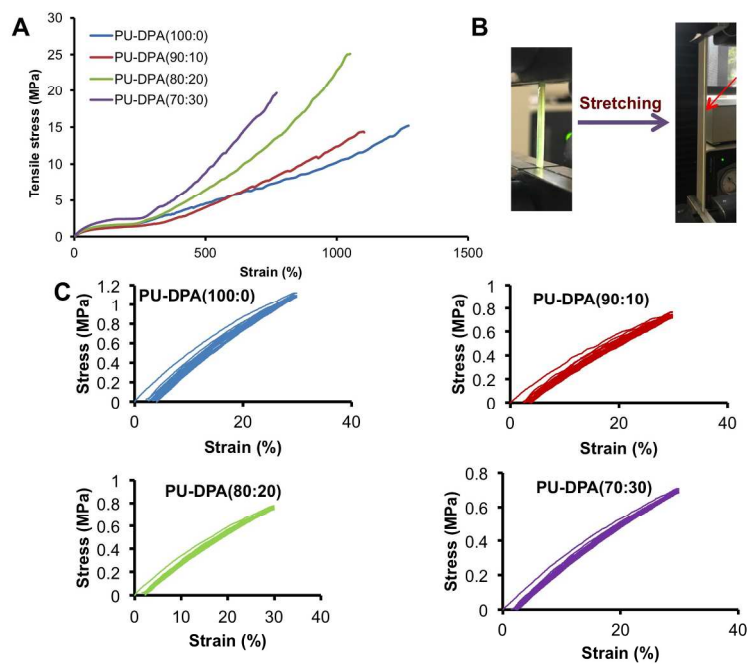


**Figure 3**

Figure 3. Mechanical properties of PU-DPA. (A) Typical stress-strain curves of PU-DPA films. (B) Images to show the PU-DPA(70:30) film is highly stretchable. (C) Cyclic stretching curves of PU-DPA polymers at 30% strain to exhibit their high elasticity.

874x656mm (72 x 72 DPI)

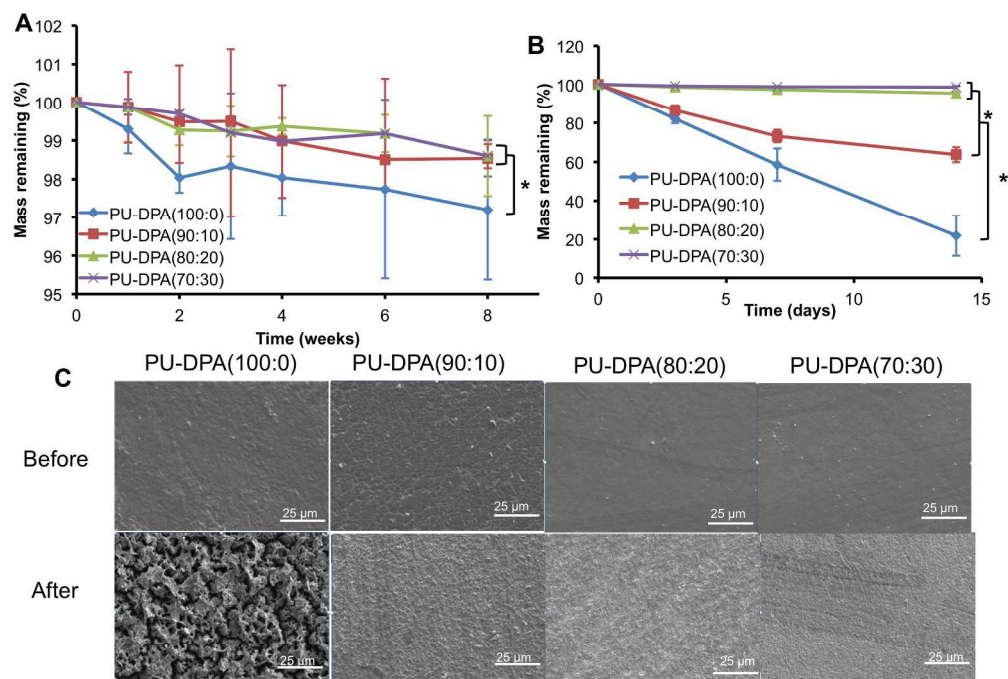


**Figure 4**

Figure 4. Mass remaining for PU-DPA films ( $n=3$ ) in (A) PBS up to 8 weeks and (B) 100 U/mL lipase/PBS up to 14 days at 37 °C. \* represents significantly different groups ( $p < 0.05$ ). (C) SEM images of the surface morphologies of PU-DPA films before and after enzymatic degradation for 14 days.

874x656mm (72 x 72 DPI)

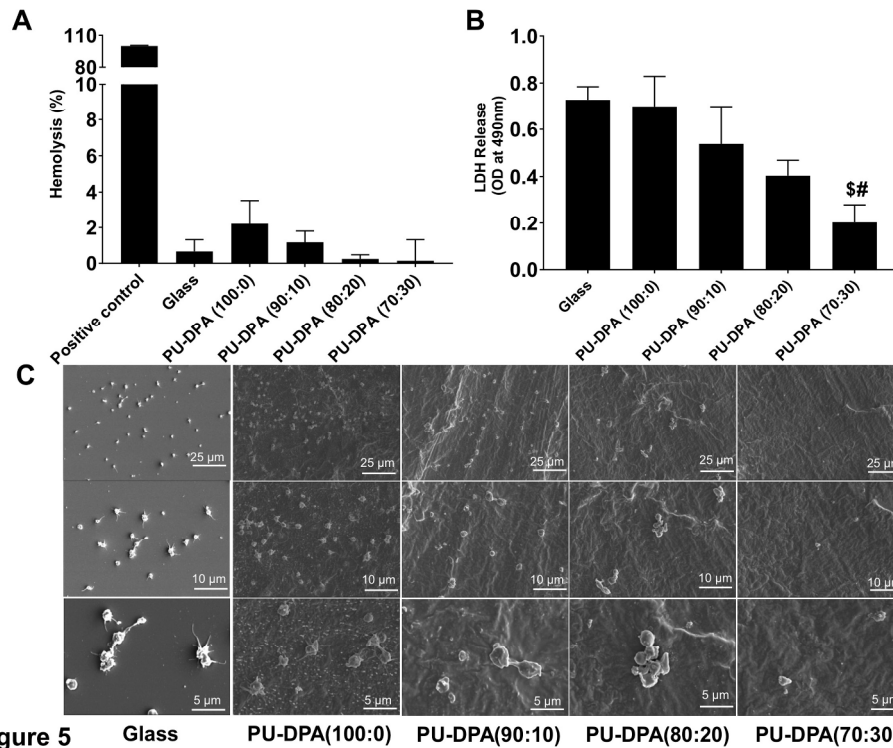
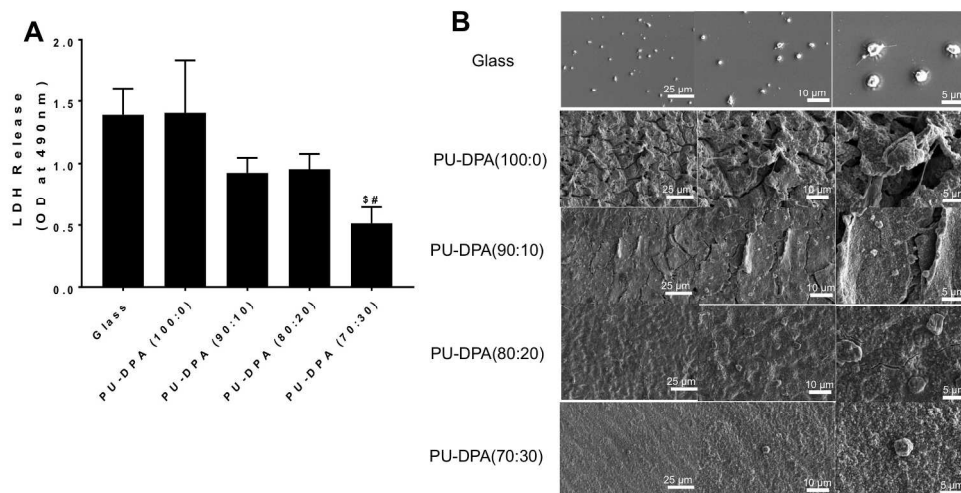


**Figure 5** Glass PU-DPA(100:0) PU-DPA(90:10) PU-DPA(80:20) PU-DPA(70:30)

Figure 5. Hemocompatibility assessment of PU-DPA films. (A) Percentage of red blood cells lysis after 2-hour exposure of whole blood with PU-DPA films ( $n = 4$ ). DI water and saline diluted blood served as positive and negative controls, respectively. Glass is used for a comparison for blood testing studies. (\* denotes  $p < 0.05$  for significant difference with respect to glass, PU-DPA(100:0), PU-DPA(90:10), PU-DPA(80:20) and PU-DPA(70:30)), (B) Amount of LDH released by triton treated platelets after adhering on to PU-DPA films in 1-hour incubation at 37°C ( $n=5$ , \$ and # denote  $p < 0.05$  for significant difference with respect to PU-DPA (100:0) and glass, respectively); and (C) SEM images to show platelet deposition and morphology on PU-DPA films.

874x656mm (72 x 72 DPI)

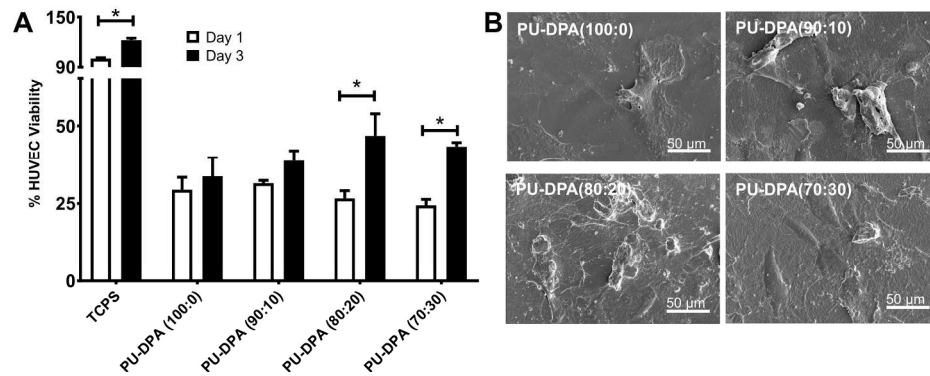




**Figure 6**

Figure 6. Blood platelets deposition on enzymatically degraded PU-DPA films. (A) Amount of LDH released by triton treated platelets deposited on PU-DPA films after 1-hour incubation at 37°C (n=5, \$ and # denote  $p < 0.05$  for significant difference with respect to PU-DPA (100:0) and glass, respectively); and (B) SEM images to show platelet deposition and morphology on enzymatically degraded PU-DPA films (14 days).

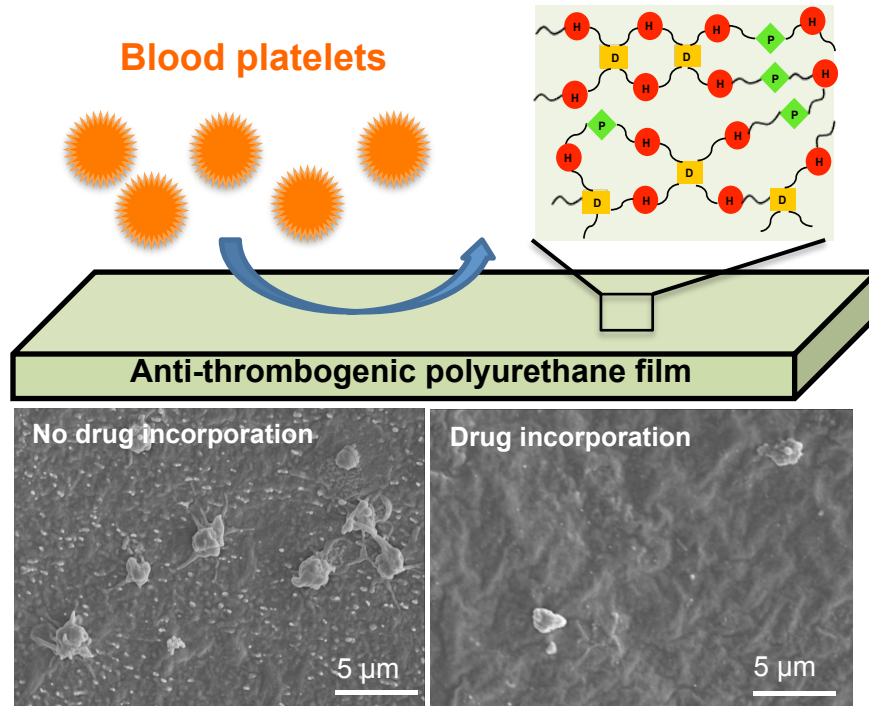
874x656mm (72 x 72 DPI)



**Figure 7**

Figure 7. In vitro HUVEC growth on PU-DPA films. (A) Cell viability measured by MTS assay to show HUVECs growth on the surfaces of PU-DPA films up to 3 days ( $n = 4$ ). TCPS surface served as the control. (B) SEM images showed HUVECs morphology on surfaces of PU-DPA films at day 3. (\* denotes  $p < 0.05$  for significant difference within the groups after 1 and 3 days of culture).

874x656mm (72 x 72 DPI)



An anti-thrombogenic, elastic, biodegradable polyurethane with covalently incorporated drug can reduce blood platelet deposition on the surface.